JOURNAL OF MATERIALS SCIENCE 26 (1991) 2913–2920

Effect of a high-temperature cycle on the mechanical properties of silicon carbide/titanium metal matrix composites

R. A. NAIK, W. D. POLLOCK
Analytical Services and Materials, Inc., Hampton, VA, USA
W. S. JOHNSON
NASA Langley Research Center, MS 188E, Hampton, VA 123665-5225, USA

The effects of fibre/matrix interface strength and thermal residual stresses on the mechanical properties of a silicon carbide/titanium composite were investigated. A 3-ply [0/90/0] composite was subjected to a simulated superplastic forming/diffusion bonding (SPF/DB) temperature cycle which changed fibre/matrix interfacial strength and thermal residual stresses in the composite. The [0/90/0] composite subjected to the SPF/DB process showed a 25% decrease in ultimate tensile strength (UTS) and a 30% decrease in failure strain compared to the as-fabricated (ASF) material. The fatigue life for the SPF/DB specimens was approximately 50% lower than the ASF specimens. The fracture surface of the ASF specimens was very irregular accompanied by substantial fibre pull-out as compared to the planar fracture surface of the SPF/DB cycled specimens that showed negligible fibre pull-out. The large changes in the tensile strength and fatigue life due to the SPF/DB cycle are explained by a difference in the failure mechanisms occurring as a result of the SPF/DB-induced changes in the strength of the fibre/matrix interface and higher thermal residual stresses. Unreinforced titanium was also tested to study the effect of the SPF/DB cycle on the matrix static properties. Fibres were etched from the composite and then individually tested for modulus and strength. Finally, a microscopic examination of the fibre/matrix interface was performed to study the effects of the SPF/DB cycle on the interface.

1. Introduction

Titanium matrix composites reinforced with continuous silicon carbide (SCS-6) fibres are of current interest as structural materials for high-temperature applications. Some of the potential applications of these composites are the National Aerospace Plane, aircraft engines, the Advanced Tactical Fighter and other high-speed aircraft. These titanium matrix composites may be diffusion bonded to a superplastically formed titanium truss core substructure. In such a process, the titanium matrix composites would be subjected to the temperature/time cycle associated with the superplastic forming/diffusion bonding (SPF/DB) process. A major concern is the change in the fibre/matrix interface strength and the thermal residual stresses as a result of this thermal cycle and the consequent effects on composite properties. The present study investigates the changes in interface strength and thermal residual stresses and their effect on the mechanical properties of a 3-ply [0/90/0] SCS-6/Ti–15V–3Cr–3Al–3Sn (referred to as SCS-6/Ti–15–3) laminate after exposure to a simulated SPF/DB cycle.

Several investigators [1, 2] have previously reported relevant results for laminates subjected to a similar thermal processing cycle. Harmon *et al.* [1] studied the static properties of $(B_4C)B$/Ti–15–3 that had been subjected to a simulated SPF/DB cycle in which the composite is kept at 1000 °C for 1 h. They found a significant (over 35%) reduction in static strength as a result of the SPF/DB cycle for this boron/titanium composite. Kaneko and Woods [2] studied the effect of a simulated braze cycle (peak temperature of 690 °C) on the static strength of unreinforced titanium. The tensile strength of the Ti–15–3 was reduced about 7% by the thermal processing. An understanding of the failure mechanisms and the changes in the composite, its constituents and the fibre/matrix interface as a result of the SPF/DB cycle was lacking.

The objective of the present study was to show how the fibre/matrix interface strength and thermal residual stresses can influence the mechanical properties of a SCS-6/Ti–15–3 composite. Composite specimens were tested under static loading to study the effect of the simulated SPF/DB cycle on the modulus and strength. Unreinforced Ti–15–3 was also tested to study the effect of the SPF/DB cycle on the matrix static properties. Next, the effect of the SPF/DB cycle on the fatigue response and failure modes of the

0022–2461/91 $03.00 + .12

composite was investigated. Fibres removed from the two panels by dissolving the titanium matrix were then individually tested for modulus and strength. Finally, a detailed microscopic examination of the fibre/matrix interface was performed to study the effects of the SPF/DB cycle on the interface.

2. Experimental procedure

2.1. Materials and specimens

Ti–15V–3Cr–3Al–3Sn is a metastable beta titanium alloy [3]. SCS-6 fibres are silicon carbide fibres that have a carbon core and a thin carbon-rich surface layer [4]. The typical fibre diameter is 0.142 mm. The composite laminates were made by hot-pressing Ti–15–3 foils between unidirectional tapes of SCS-6 fibres. For the present study, two panels with a 3-ply [0/90/0] layup were used. Laminate thickness was approximately 0.68 mm. The fibre volume fraction was measured as 0.375.

One of the panels was tested in the as-fabricated (ASF) condition. A second panel was subjected to a thermal processing cycle that simulated only the time–temperature portion of an SPF/DB bonding operation. This simulated SPF/DB cycle was performed in a vacuum furnace and consisted of raising the temperature from ambient to 700 °C at a rate of 10 °C min^{-1}. After stabilizing at 700 °C the temperature was further increased to 1000 °C at a rate of 4 °C min^{-1}. The panel was held at 1000 °C for 1 h. It was then furnace cooled to 594 °C at a rate of 8 °C min^{-1} and held at that temperature for 8 h. Finally, it was furnace cooled to 150 °C and held for about 10 h before cooling to ambient temperature.

Each panel was cut into 19 mm × 152 mm rectangular specimens using a diamond wheel saw. These specimens were then "dog-boned", as shown in Fig. 1, using electro-discharge machining. One rectangular reinforced titanium specimen (12.7 mm × 152 mm) that had been subjected to the SPF/DB cycle was also tested. This unreinforced titanium specimen was, in fact, a "fibreless composite" and was made by consolidating Ti–15–3 foils by the same temperature–time–pressure cycle used for the composite laminates.

2.2. Specimen testing

Tests were conducted in a servo-hydraulic test stand under load control with a loading rate of 45 N s^{-1}. The 0° fibres were parallel to the loading direction in all cases. The specimens were strain-gauged for moduli determination under static loading. An extensometer was used to measure the axial strain of the fatigue specimens. All fatigue specimens were tested at an R ratio of 0.1 and at a frequency of 10 Hz. A digital data acquisition system was used to collect load and stain data. All tests were performed at room temperature.

2.3. Fibre testing

The effect of the SPF/DB cycle on the fibre properties was determined by testing single fibres from each

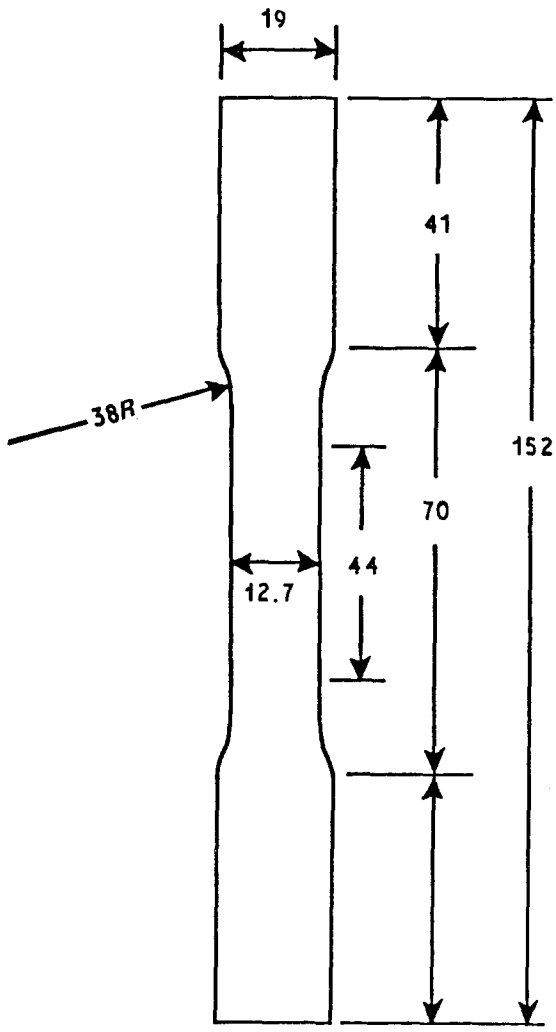

Figure 1 Dog-bone specimen and dimensions (mm).

panel. Thin strips, 3.2 mm wide, were cut from the ASF and the SPF/DB cycled panels. These strips were then dipped into a bath of acid to dissolve all the titanium. Two different acids, hydrofluoric and bromine etch, were used to study the effect of the etching on the fibre properties. The bromine etch consisted of a solution of 10% bromine and 90% methanol mixed with 10 mg tartaric acid. The bare fibres were tested individually in a screw-driven machine. A single fibre was mounted between a special fixture for ease of handling and gripping as per ASTM Standard D 3379-75 [5]. The fibre was tested to failure while the load and crosshead displacement were recorded on an X–Y plotter and a computer-controlled data acquisition system. The fibre diameter was measured using an optical microscope and was typically 0.142 mm. Typical gauge length of the fibres tested was 75 mm. Fibre modulus and strength were determined from the recorded data as per ASTM Standard D 3379-75 [5].

3. Results and discussion

This section presents the experimental results for the composite and its constituents. First, the effect of the SPF/DB cycle on the static and fatigue properties of the composite and the observed failure modes for the ASF and the SPF/DB cycled panels are presented.

Next, a microscopic examination of the failure surfaces is presented. Then, the results of tests on the matrix material and individual fibres is presented to assess the effect of the SPF/DB temperature cycle on the composite's constituent properties. Next, a microstructural analysis of the fibre/matrix interface for the ASF and the SPF/DB cycled panels is presented. Lastly, a description of the failure process is given to explain the differences in mechanical properties of the ASF and SPF/DB composite materials.

3.1. Composite properties

The mechanical properties, under static tension, were determined from at least three specimens cut from each panel. The specimens cut from the SPF/DB cycled panel showed a 9% increase in modulus but a 25% decrease in UTS and a 30% decrease in failure strain as compared to the ASF specimens (see Table I). Under cyclic fatigue ($R = 0.1$ at 10 Hz), the SPF/DB cycled specimens showed a significant reduction (over 50%) in the fatigue life (Fig. 2) as compared to the ASF specimens. In order to study the reasons for the lower UTS and fatigue properties of the SPF/DB cycled specimens, a microscopic study was performed.

The fracture surfaces for the statically tested ASF and SPF/DB cycled specimens were significantly different as shown in Fig. 3. The ASF fracture surfaces were in general more irregular than those of the SPF/DB cycled specimens. There was more fibre pull-out in the ASF specimens than in the SPF/DB cycled specimens where the fibres appeared to be almost flush with the fracture surface. The rough fracture surface on the ASF specimens indicates that the crack had to take a tortuous path as it progressed through the composite debonding the fibre/matrix interface as it progressed. The relatively smooth fracture surface

TABLE I Static properties of ASF and SPF/DB [0/90/0] composite panels

	Modulus (GPa)	Poisson's ratio	UTS (MPa)	Failure strain
ASF panel	156	0.21	1070	0.0105
SPF/DB panel	170	0.33	805	0.0073

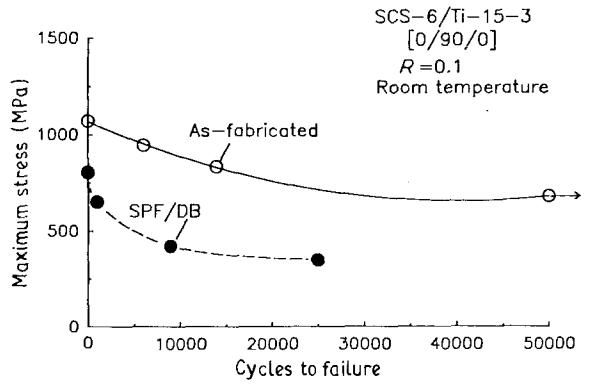

Figure 2 *S–N* curves for ASF and SPF/DB [0/90/0] SCS-6/Ti-15-3 laminates.

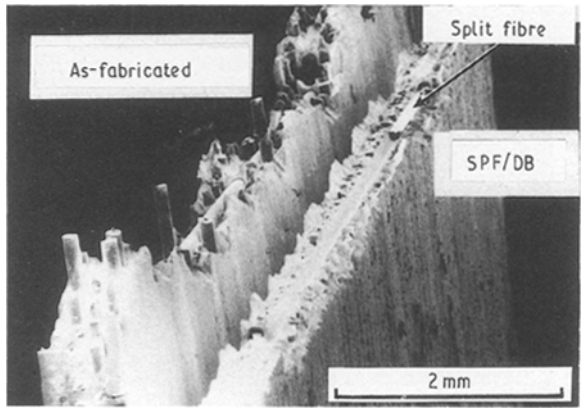

Figure 3 Fracture surface morphology for statistically tested specimens, SCS-6/Ti-15-3 [0/90/0].

on the SPF/DB cycled specimens indicates that the crack did not deviate along the 0° fibre length but broke fibres as it grew. Also, notice the split fibre in the 90° (transverse) ply. This split fibre was typically observed in the SPF/DB cycled specimens but not in the ASF specimens. The fracture surfaces of the fatigue specimens were similar to those observed for the static specimens from each panel type.

The effect of the SPF/DB cycle on the matrix, fibre and/or the fibre/matrix interface might explain these large differences in fracture surface morphology and also the differences in strength and fatigue resistance.

3.2. Unreinforced Ti-15-3 properties

The Ti-15-3 properties were obtained from tests conducted on the "fibreless composite" described earlier. The stress–strain curves for the ASF, SPF/DB cycled and peak aged Ti-15-3 are shown in Fig. 4. The ASF and aged (482 °C for 16 h) properties were reported previously [6]. The stress–strain curve for the SPF/DB cycled specimen lies in between the curves for the ASF and aged conditions. The SPF/DB cycled specimen, under static tension, showed a 9% increase in modulus and ultimate tensile strength (UTS) and a 9% decrease in the strain to failure as compared to the as-fabricated Ti-15-3. The peak aged specimens

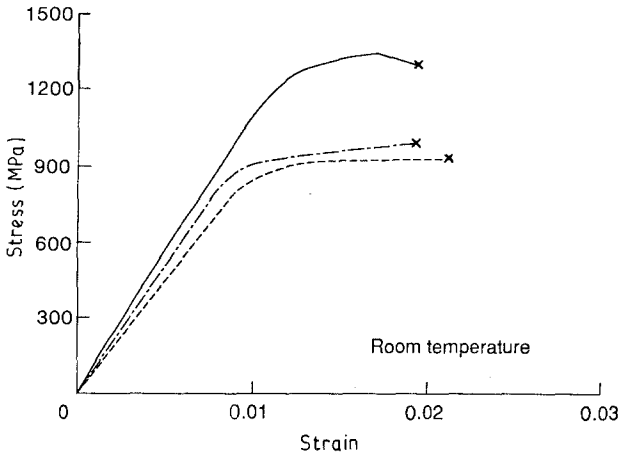

Figure 4 Unreinforced Ti-15-3 stress–strain curves at room temperature. (×) Specimen failure (— — —) SPF/DB cycled, (——) aged [6], (– – –) as-fabricated [6].

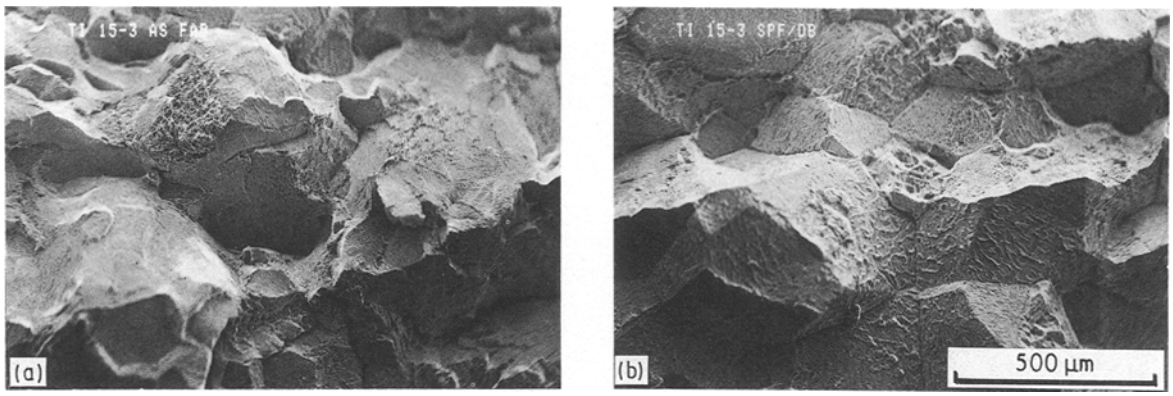

Figure 5 Electron micrographs of Ti–15–3 fracture surfaces. (a) ASF, (b) SPF/DB.

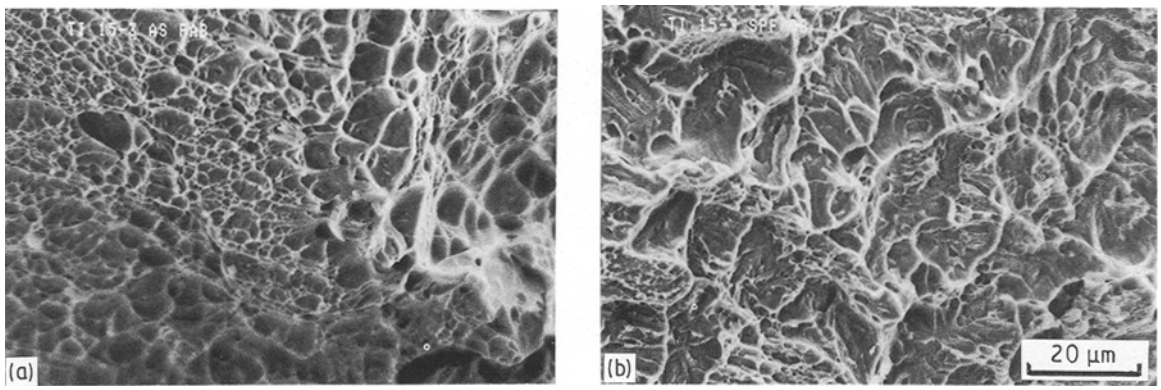

Figure 6 High-magnification micrographs of Ti–15–3 fracture surfaces. (a) ASF, (b) SPF/DB.

showed a 17% increase in modulus and a 44% increase in UTS as compared to the as-fabricated specimens. Thus, the SPF/DB cycle did not change matrix properties as much as peak ageing.

The coefficient of thermal expansion (CTE) of the matrix in the ASF and the SPF/DB condition was also measured. The measured CTE for the ASF material compared well with the data in [3]. The CTEs for the ASF and the SPF/DB material were, within experimental error, the same.

Fractographic studies were conducted on the failure surfaces of both the ASF and SPF/DB matrix material. Low and high magnification micrographs of the fracture surfaces are shown in Figs 5 and 6. The ASF failure surface was characterized by intergranular/transgranular mixed mode failures. The dimples in the ASF specimen resulted from ductile failure (microvoid nucleation, growth, and coalescence). The SPF/DB specimen also displayed a mixed mode failure surface, although more of it appeared to be intergranular. The significant difference between the two materials is apparent at the higher magnification (Fig. 6) where quasi-cleavage is observed. Quasi-cleavage is brittle cleavage combined with ductile dimples. Fractography on the SPF/DB material shows that it is more brittle than the ASF material. This correlates well with the lower strain to failure for the SPF/DB specimens as compared to the ASF specimens (see Fig. 4).

3.3. Fibre properties

Single fibre tests were performed on fibres that were etched away from the two panels. As mentioned earlier, two different acids were used for the etching in order to study the effect of the etching on the fibre properties. At least three fibres were tested from each panel and for each etching technique. UTS for fibres from the ASF and SPF/DB cycled panels etched using hydrofluoric acid (HF) were 3.55 ± 0.3 GPa and 3.8 ± 0.25 GPa, respectively. Failure strains for these fibres from the ASF and SPF/DB cycled panels were 0.011 ± 0.002 and 0.013 ± 0.003, respectively. The longitudinal modulus for the HF etched fibres from the ASF and SPF/DB cycled panels were 405 ± 11 GPa and 389 ± 15 GPa, respectively. Fibres etched using the mild bromine acid had, approximately, the same strength and modulus as those etched using the harsher hydrofluoric acid. Typical fibre moduli for the SCS-6 fibres are 400 GPa [6]. Thus, the SPF/DB cycle did not seem to affect the fibre properties significantly.

3.4. Fibre/matrix interface and residual stresses

The differences between the mechanical properties of the ASF and SPF/DB specimens cannot be explained

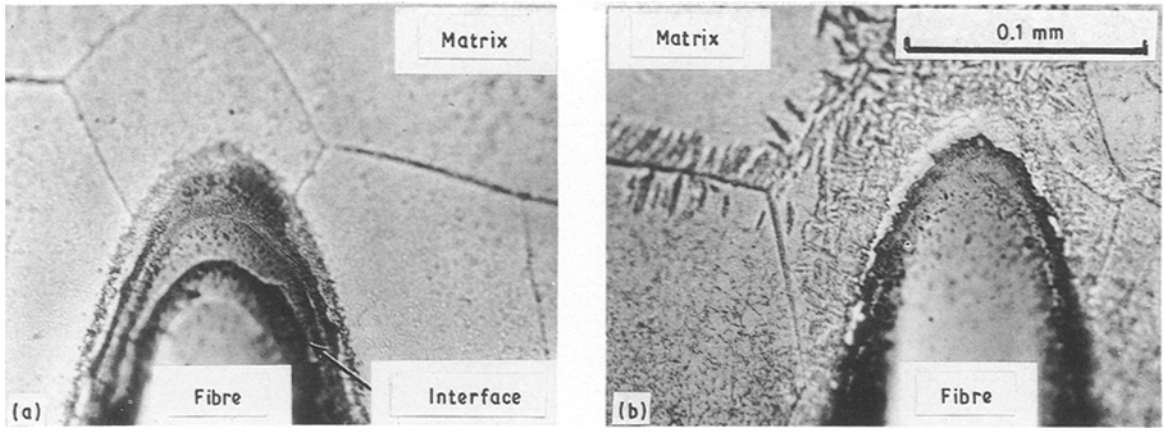

Figure 7 Micrographs of the fibre/matrix interface region. (a) ASF, (b) SPF/DB.

by the observed changes in the fibre or matrix properties. Therefore, the present section will describe the results of a microstructural analysis of the fibre/matrix interface in the ASF and SPF/DB cycled panels and show how the composite stress–strain response can be used to assess the strength of the fibre/matrix interface [6] and the relative level of residual thermal stresses.

The ASF specimens show an irregular fracture surface with significant fibre pull-out and the SPF/DB cycled specimens show a flat fracture surface with flush fibre ends. The evidence of split 90° fibres in the SPF/DB cycled specimens (Fig. 3) also suggests that the interface was sufficiently strong to transmit enough load into the fibre to cause it to split. It is assumed that the interface in the ASF specimen was not as strong because no split 90° fibres were observed.

The fibre/matrix interfaces, as shown in Fig. 7, are significantly different between the ASF and SPF/DB cycled panels. The optical micrographs in Fig. 7 were obtained from oblique sections of the composite in order to exaggerate the fibre/matrix interface region. The specimens were etched with a solution of 100 ml H_2O, 6 ml HNO_3, and 3 ml HF. The ASF section has a layered interface region, whereas in the SPF/DB cycled section the titanium appears to have reacted with the carbon and the silicon, as a result of the high-temperature SPF/DB cycle. An acicular alpha phase forms along grain boundaries in the SPF/DB material. This alpha phase is more brittle compared to the beta phase. The fibre/matrix interfaces were also studied using an electron microprobe. The microprobe scans are presented in Fig. 8. The line scans show the distribution of the elements across to the interface before and after the thermal cycle. The scan for C in the ASF material has two peaks in the interface region. These peaks correspond to the two step deposition of C-rich regions on the surface of the SCS-6 fibre during manufacture. The valley between the peaks corresponds to a peak in the Si scan due to an increase in the Si deposition rate between the C-rich layers. The gradients of the Ti and Si scans are quite steep, indicating that there is little inter-diffusion of these two elements. In contrast, the Si and Ti scans in the SPF/DB specimen show a gradual gradient,

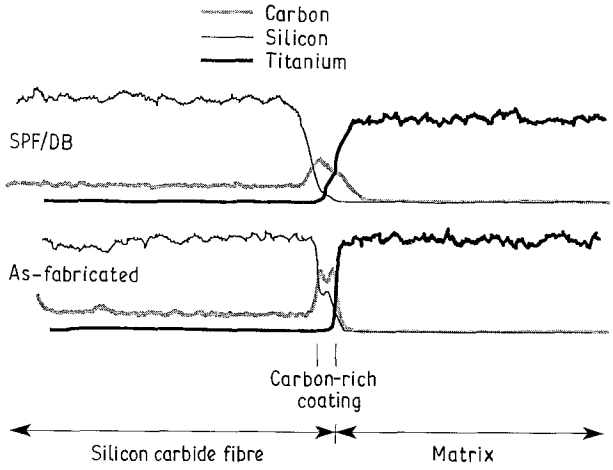

Figure 8 Electron microprobe elemental line scan for SCS-6/Ti–15–3.

indicating that there has been greater inter-diffusion. In addition the dual peaks in the C scan are absent and the C-rich region appears thicker and extends into the matrix. The inter-diffusion of the C, Ti and Si would presumably form brittle titanium carbides and titanium silicides. These thicker, brittler reaction zones could serve to increase the stress concentration at the fibre surface, thus enhancing the probability of fibre failure directly ahead of an advancing matrix crack.

Fig. 9 shows close-up views of the same failure surfaces that were shown in Fig. 3 with the 0° fibres coming out of the paper. The region between the two 0° plies is a channel left behind by a 90° fibre that was pulled away. In the ASF specimen this channel appears to have a single uniform texture indicating a clean break at the fibre/matrix interface. That is, a clear single plane of weakness at one of the interfaces shown in Fig. 7. The channel in the SPF/DB cycled specimen shows at least two different textures indicating that there was not a single plane of weakness.

Fig. 10 gives a typical stress–strain response for the SPF/DB cycled specimens. The formation of a knee in the stress–strain curve at stress levels well below the yield stress of the matrix is typical of SCS-6/Ti–15–3 composites. Johnson *et al.* [6] observed this knee for a

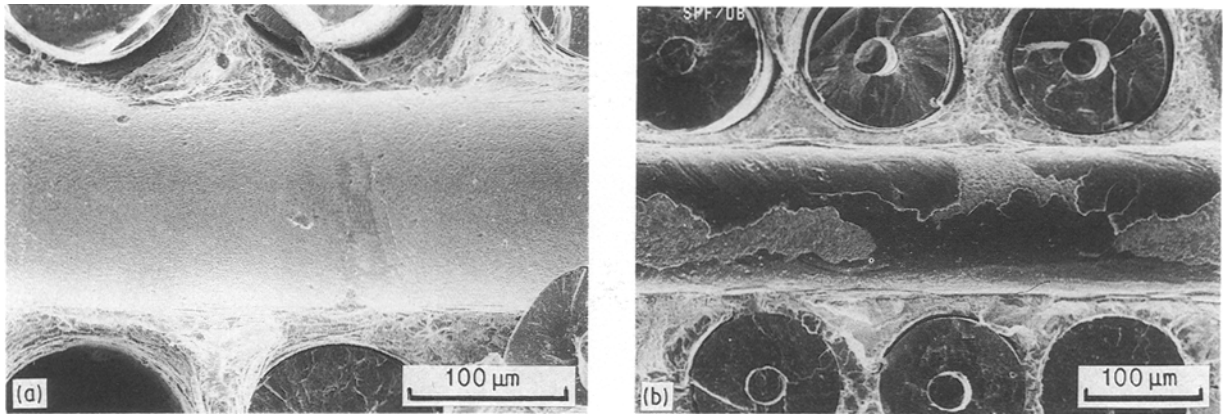

Figure 9 Micrograph showing channel left behind by a pulled out fibre. (a) ASF, (b) SPF/DB cycled.

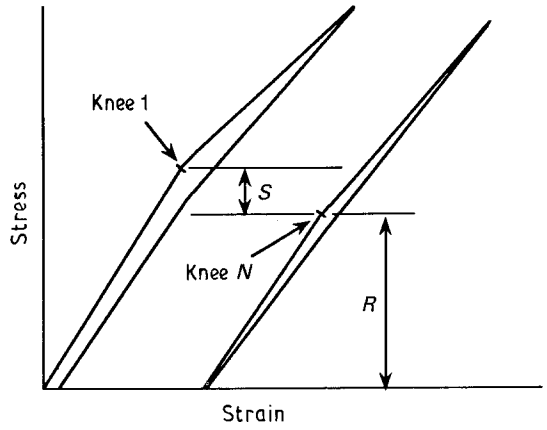

	Knee 1	Knee *N*	*S*
ASF	67 MPa	46 MPa	21 MPa
SPF/DB	123 MPa	86 MPa	37 MPa

Figure 10 Typical stress–strain curves for SCS-6/Ti–15–3 [0/90/0] specimens, where *S* is the interface strength, and *R* is the residual stress.

range of composite layups and attributed the formation of the knee to the failure of the fibre/matrix interface in the off-axis plies. After the first loading–unloading cycle, a knee is observed on each subsequent cycle but at a lower stress level than the first cycle. As noted in [6], the knee on the first loading–unloading cycle corresponds to failure of the fibre/matrix interface. In order to fail the interface considerable compressive radial stresses and tensile tangential stresses around the fibre must be negated by the applied loading. During the subsequent load cycles only the residual stresses must be overcome to cause fibre/matrix separation because the fibre/matrix interface has already been broken. The difference in the knee stress levels between the first and the subsequent cycles (*S*, Fig. 10) is, therefore, an indicator of the strength of the fibre/matrix interface in the off-axis plies. The stress level of the knee in the subsequent cycles (*R*, Fig. 10) is proportional to the level of the thermal residual stresses. Fig. 10 also shows the measured values of *S* and the level of the subsequent knees (knee *N*) for both the ASF and SPF/DB specimens. From the *S* values we can imply that the fibre/matrix interface is 50% stronger in the SPF/DB material. From the knee *N* data, the thermal residual stresses appear to increase almost 100% due to the SPF/DB temperature cycle.

A simple finite element micromechanics analysis [8] indicates that the residual compressive radial stresses around the fibre will be 9% higher just due to the increase in the matrix modulus. This analysis shows a trend in right direction but does not completely explain the differences in the measured knees in the stress–strain curves.

3.5. Failure mechanisms

The large differences in the UTS (Table I) and fatigue strength (Fig. 2) of the ASF and SPF/DB cycled panels cannot be explained by the small differences in matrix and fibre properties. Also, the differences in the failure surfaces of the two specimen types (Fig. 3) cannot be explained by differences in the fibre and matrix properties. The present section explains how differences between the fibre/matrix interfaces and thermal residual stresses can explain the differences in the failure surfaces and in the UTS and fatigue life.

In the case of a fatigue crack that initiates in the matrix and encounters the fibre/matrix interface, it can either break the fibre and move ahead or it can debond the fibre/matrix interface for some distance and grow around the fibre. In the ASF specimens a crack that reaches a 0° fibre finds a path of less resistance along the weaker fibre/matrix interface and starts debonding along the length of the fibre for some distance. This progression of damage along the fibre/matrix interfaces dissipates much energy. The crack continues to grow in such a manner until one of the fibres left behind is loaded to failure. Such a scenario is illustrated in Fig. 11. The stronger and stiffer the matrix material, the higher is the stress concentration at a matrix crack tip. The SPF/DB matrix material is approximately 9% stronger and stiffer than the ASF matrix material. In the SPF/DB cycled specimens, with the stronger and brittler interface, the matrix crack which reaches the interface does not debond the fibre/matrix interface, but instead breaks the fibre

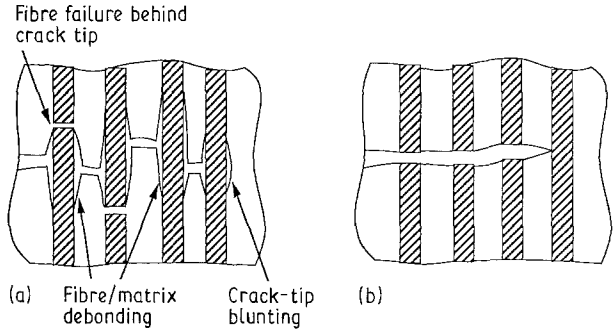

Figure 11 Failure mechanisms in 0° ply for (a) ASF and (b) SPF/DB [0/90/0] laminates.

when the stress intensity at the crack tip reaches a critical value. Also, the higher the residual thermal stresses are around the fibre the more difficult the fibre/matrix debonding will be. Recall that the residual compressive radial stress around the fibre in the SPF/DB material was found to be twice that in the ASF material.

According to a shear-lag analysis by Goree and Gross [9] the stress concentration in the first unbroken fibre in the crack path is over 35% lower for the ASF failure scenario than for the SPF/DB scenario shown in Fig. 11. This assumes the same crack length and loading in each case. This implies that an applied load would have to be approximately 35% higher in the ASF material than in the SPF/DB material. This is very close to the 25% increase in static strength that was found. Not only is the stress concentration in the fibres lowered by the fibre/matrix debonding but more internal energy is dissipated, particularly by internal friction during fatigue. The compressive radial stresses and the tensile hoop stresses, due to cooldown, at the fibre/matrix interface cause a "choking" of the fibre by the matrix leading to high frictional stresses during fatigue. Even after the fibre/matrix interface has been debonded the elastic residual stresses still act to "choke" the fibre. Thus as the crack opens and closes during fatigue, considerable friction is expected to exist between the fibre and the debonded matrix.

Thus we have explained how the failure mechanisms are influenced by the changes in fibre/matrix interface strength and the residual thermal stresses. This difference in the internal stress state affects the failure mechanisms resulting in significant changes in static and fatigue strength.

4. Conclusion

The changes in the fibre/matrix interface as a result of a simulated superplastic forming/diffusion bonding (SPF/DB) temperature cycle on a 3-ply [0/90/0] SCS-6/Ti–15V–3Al–3Cr–3Sn composite were investigated. The composite showed a 9% increase in modulus but a 25% decrease in UTS and a 30% decrease in failure strain as a result of the SPF/DB process. The fatigue endurance limit for the SPF/DB cycled specimens was 50% lower than the ASF specimens. The fracture surface of the ASF specimens was very irregular with significant fibre pull-out as compared to the planar fracture surface of the SPF/DB cycled specimens where fibre ends were flush with the surface.

The fibres leached from the ASF and SPF/DB cycled panels were only marginally different as a result of the high-temperature cycle. Matrix-only SPF/DB specimens showed a 9% increase in modulus and ultimate tensile strength as compared to the ASF specimens. The large changes in the UTS, the fatigue life, and the fracture surfaces due to the SPF/DB cycle are believed to be a result of changes in the strength of the fibre/matrix interface and the residual radial stresses around each fibre. A stronger interface in the SPF/DB cycled specimens leads to higher stress intensities at the fibre resulting in early fibre failures. The weaker interface in the ASF specimens results in fibre/matrix debonds running along the length of the fibres and thereby dissipating more energy and lowering stress intensities at the fibres. This results in fibre failures at much higher loads. The fracture surfaces of the ASF and SPF/DB cycled specimens are consistent with these different failure mechanisms.

Optical microscopy of the fibre/matrix interface revealed a multi-layered interface in the ASF composite. The SPF/DB cycle altered the multi-layered interface. In both cases, the stress–strain response showed a knee typical of off-axis fibre/matrix interface failure. Differences between the first and subsequent knees for the SPF/DB cycled specimens and the ASF specimens suggested the SPF/DB cycle strengthened the fibre/matrix interface. Differences between appearances of the fracture surfaces were consistent with differences between interface strengths.

In short, for the laminates in question, the SPF/DB cycle apparently increased the matrix strength and modulus, had little or no effect on fibre strength and modulus, but significantly reduced both the static and fatigue strength of the laminate. This strength reduction is primarily due to an elevation of residual radial compressive stresses in the matrix around the fibres and an apparently stronger interfacial bonding between the fibre and matrix.

Acknowledgement

The [0/90/0] panels were supplied to the NASA Langley Research Center by the McDonnell Douglas Corporation.

References

1. D. M. HARMON, C. R. SAFF and C. T. SUN, "Durability of Continuous Fiber Reinforced Metal Matrix Composites", AFWAL-TR-87-3060 (October 1987).
2. R. S. KANEKO and C. A. WOODS, "Low-Temperature Forming of Beta Titanium Alloys", NASA Contractor Report 3706 (September 1983).
3. H. W. ROSENBERG, *J. Metals* **35**(11) (1986) 30.
4. F. E. WAWNER Jr, "Boron and Silicon Carbide/Carbon Fibres", in "Fibre Reinforcements for Composite Materials", edited by A. R. Bunsell (Elsevier Science, Amsterdam, 1988) pp. 371–425.
5. "1987 Annual Book of ASTM Standards", Section 15, Vol. 15.03 (American Society for Testing and Materials, Philadelphia, 1987) pp. 181–86.

6. W. S. JOHNSON, S. J. LUBOWINSKI and A. L. HIGHSMITH, "Mechanical Characterization of SCS-6/Ti–15–3 Metal Matrix Composites at Room Temperature", in Thermal and Mechanical Behavior of Metal Matrix and Ceramic Matrix Composites", ASTM STP 1080, edited by J. M. Kennedy, H. H. Moeller and W. S. Johnson (American Society for Testing and Materials, Philadelphia, 1990) pp. 193–218.
7. W. S. JOHNSON, "Fatigue Testing and Damage Development in Continuous Fiber Reinforced Metal Matrix Composites", in Metal Matrix Composites: Testing, Analysis and Failure Modes", ASTM STP 1032, edited by W. S. Johnson (American Society for Testing and Materials, Philadelphia, 1989) pp. 194–221.
8. A. L. HIGHSMITH, D. SHIN and R. A. NAIK, "Local Stresses in Metal Matrix Composites Subjected to Thermal and Mechanical Loading", in "Thermomechanical Behavior of Metal and Ceramic Matrix Composites", ASTM STP 1080, edited by J. M. Kennedy, H. H. Moeller and W. S. Johnson (American Society for Testing and Materials, Philadelphia, 1990) pp. 3–19.
9. J. G. GOREE and R. S. GROSS, *Engng Fract. Mech.* **13** (1979) 563–578.

Received 2 January
and accepted 4 September 1990